Analyzing Photonic Crystal Waveguides by Dirichlet-to-Neumann Maps

Yuexia Huang, Ya Yan Lu and Shaojie Li

Department of Mathematics, City University of Hong Kong, Kowloon, Hong Kong

An efficient numerical method is developed for modal analysis of two-dimensional photonic crystal waveguides. Using the Dirichlet-to-Neumann (DtN) map of the supercell, the waveguide modes are solved from an eigenvalue problem formulated on two boundaries of the supercell, leading to significantly smaller matrices when it is discretized. The eigenvalue problem is linear even when the medium is dispersive. The DtN map of a domain is an operator that maps the wave field on the boundary of the domain to the normal derivative of the field. The DtN map of the supercell can be efficiently calculated by merging the DtN maps of the ordinary and defect unit cells.

OCIS codes: 050.5298,130.5296,000.4430

1. Introduction

In recent years, photonic crystals (PhCs) [1–3] have been extensively studied due to their significant potential in realizing high density photonic integrated circuits. The periodic variation of the refractive index in a PhC gives rise to bandgaps, i.e., frequency intervals in which the propagation of light is forbidden. These bandgaps make it possible to design photonic crystal waveguides (PCWs) by introducing line defects in an otherwise periodic PhC structure. Comparing with conventional optical waveguides, PCWs have the advantage of low loss and high confinement, and they can be used to bend light on the wavelength scale [4].

Efficient numerical methods are important to the design and optimization of PCWs and other PhC devices. For a straight PCW, which is still periodic along its axis, the fundamental problem is to calculate the dispersion relationships between the angular frequency ω and the Bloch wavenumber β of the propagating modes. Both time domain and frequency domain methods have been used to analyze PCWs. While the time domain methods [5–7] are quite popular, the problem is more naturally formulated in the frequency domain. Many numerical methods have been developed in the frequency domain and they follow two different approaches. In the first frequency domain approach [3], the modes are solved as an

eigenvalue problem where ω^2 is the eigenvalue and β is a given parameter. This is a linear eigenvalue problem if the medium is non-dispersive, and it is formulated on a domain Ω that covers one period of the structure along the waveguide axis. If y is the axis of the PCW and L is the period in y, then Ω is the domain given by $0 < y < L$. Many numerical methods, including the plane wave expansion method [8–10], the finite difference method [11] and the finite element method, have been developed using this approach. In fact, most existing methods [12–23] for PhC band structures can be used to calculate PCW modes if the unit cell of the original PhC is replaced by the domain Ω. In practice, the unbounded transverse directions of Ω must be truncated, but even the truncated domain is much larger than the unit cell of the original PhC. Therefore, the numerical methods based on this approach give rise to matrices that are much larger than those for band structure calculations. Furthermore, the frequencies of the waveguide modes correspond to interior eigenvalues that are difficult to find by iterative eigenvalue solvers. For dispersive media, the eigenvalue problem is nonlinear and more difficult to solve.

The second approach is to solve β for a fixed ω. If it is considered on domain Ω, this approach gives rise to a linear eigenvalue problem with eigenvalue β even when the medium is dispersive [24]. Furthermore, we can reformulate the problem to the boundary of Ω to significantly reduce the resulting computation size. Notice that the boundary of Ω are two parallel transverse planes or lines at $y = 0$ and $y = L$ for three-dimensional (3D) or two-dimensional (2D) PCWs, respectively. These reformulations lead to linear eigenvalue problems (even when the medium is dispersive) with eigenvalue $\rho = \exp(i\beta L)$, and they rely on some operators, such as the transfer matrix [25] and the scattering operators [26–29], that characterize one period of the PCW. Although the transfer matrix approach is simple, it suffers numerical instabilities related to the exponential behavior of evanescent waves. The scattering operators can be computed in a number of different ways, but they cannot be easily obtained since the transverse direction is large. In this paper, we use a formulation for 2D PCWs based on the Dirichlet-to-Neumann (DtN) map of Ω [30, 31]. The DtN map of a given domain is an operator that maps the field on the boundary of the domain to its normal derivative. It has been widely used as a non-reflecting boundary condition to reduce an unbounded physical domain to a bounded computation domain [32]. In connection with periodic waveguides, such as the PCWs considered in this paper, the DtN map of an exterior domain has been used to setup a boundary condition for truncating Ω [33, 34]. This approach gives rise to a nonlinear eigenvalue problem on the truncated domain since the boundary condition involves β. Our approach is different. We use the DtN map of the domain Ω which maps the wave field at $y = 0$ and $y = L$ to its normal derivative. In our previous work, the DtN map of a unit cell has been used to analyze 2D PhCs of finite size [35–37] and to calculate band structures [38, 39]. For PCW problems, the DtN map of the domain Ω is needed. In section

3, we develop an efficient method for calculating the DtN map of Ω by merging DtN maps of the ordinary and defect unit cells. In section 4, we illustrate the accuracy and efficiency of our method by a number of examples.

2. Eigenvalue problems

We consider pure 2D PhCs composed of infinite dielectric rods or air columns whose axes are parallel to the z-axis. The structures are invariant in the z direction. For waves propagating in the xy plane, we can separately consider the E and H polarizations. We present our method for the E polarization, but also include brief comments on the necessary modifications for the H polarization. The governing equation for the E polarization is

$$\frac{\partial^2 u}{\partial x^2} + \frac{\partial^2 u}{\partial y^2} + k_0^2 n^2 \, u = 0, \tag{1}$$

where u is the z-component of the electric field, $n = n(x, y)$ a real refractive index function, $k_0 = \omega/c$ is the free space wavenumber, ω is the angular frequency and c is the speed of light in vacuum. For a typical photonic crystal waveguide (PCW) as shown in Fig. 1, the

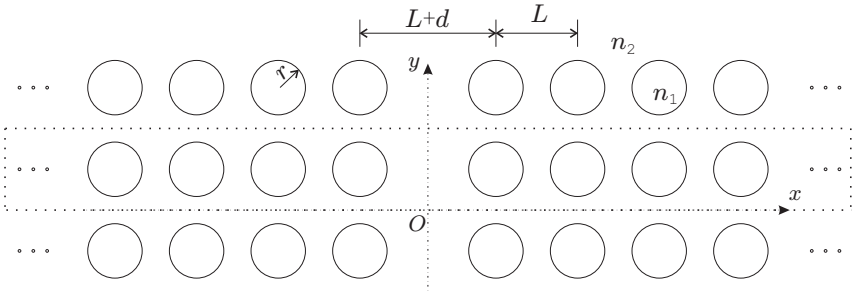

Fig. 1. A square lattice of circular rods with a line defect.

waveguide axis is the y axis and the refractive index function is periodic in y with a period L, i.e.,

$$n(x, y + L) = n(x, y). \tag{2}$$

From the Bloch-Floquet theorem, Eq. (1) has modal solutions given by

$$u(x, y) = \phi(x, y) \exp(i\beta y), \tag{3}$$

where β is the Bloch wavenumber (or propagation constant of the mode) and $\phi(x, y)$ is a periodic function of y with the same period L, i.e.,

$$\phi(x, y + L) = \phi(x, y). \tag{4}$$

From (3), we obtain the following quasi-periodic condition for u:

$$u(x, y + L) = \rho\, u(x, y), \quad \rho = \exp(i\beta L). \tag{5}$$

It also implies that

$$u(x, L) = \rho\, u(x, 0), \quad \frac{\partial u}{\partial y}(x, L) = \rho\, \frac{\partial u}{\partial y}(x, 0). \tag{6}$$

The PCW problem is formulated on one period of the structure:

$$\Omega = \{\, (x, y) \,|\, -\infty < x < \infty,\, 0 < y < L \,\}. \tag{7}$$

We can solve Eq. (1) in Ω subject to the boundary conditions (6). In the first frequency domain approach, β is assume to be a given parameter, then k_0^2 (or ω^2) is considered to be the eigenvalue. This is a linear eigenvalue problem for non-dispersive media and a nonlinear eigenvalue problem for dispersive media. The eigenvalue problem can also be given for function ϕ. We have the following equation

$$\frac{\partial^2 \phi}{\partial x^2} + \frac{\partial^2 \phi}{\partial y^2} + 2i\beta \frac{\partial \phi}{\partial y} + [k_0^2 n^2(x, y) - \beta^2]\phi = 0 \tag{8}$$

on domain Ω, and it is to be solved with the following periodic conditions:

$$\phi(x, L) = \phi(x, 0), \quad \frac{\partial \phi}{\partial y}(x, L) = \frac{\partial \phi}{\partial y}(x, 0). \tag{9}$$

The second frequency domain approach is to solve β assuming ω is a given parameter. If the problem is considered on domain Ω, then we have a quadratic eigenvalue problem where β is the eigenvalue and ϕ is the eigenfunction satisfying (8) and (9). The quadratic eigenvalue problem can be easily transformed to a linear eigenvalue problem if we double the size of the problem. For $\varphi = \partial_y \phi + i\beta\phi$, we have

$$\begin{bmatrix} \partial_y & -1 \\ \partial_x^2 + k_0^2 n^2 & \partial_y \end{bmatrix} \begin{bmatrix} \phi \\ \varphi \end{bmatrix} = -i\beta \begin{bmatrix} \phi \\ \varphi \end{bmatrix}. \tag{10}$$

Notice that φ satisfies the condition $\varphi(x, L) = \varphi(x, 0)$. Compared with the first approach where ω^2 is the eigenvalue, this formulation has the advantage of being linear even when the medium is dispersive. Furthermore, a number of reformulations exist so that the eigenvalue problem can be reduced to the boundary of Ω. For 2D PCWs considered here, the boundary of Ω comprises two transverse lines at $y = 0$ and $y = L$, respectively. In these reformulations, the eigenvalue is $\rho = \exp(i\beta L)$ and the problem is still linear.

In the scattering operator reformulation, we need to assume that the waveguide is y-invariant in a vicinity of $y = 0$ and $y = L$. Then the wave field around $y = 0$ and $y = L$ can

be decomposed as forward and backward components: $u = u^+ + u^-$. The scattering operator $\mathcal{S}$ is a 2×2 matrix, the entries of which are operators acting on functions of x, satisfying

$$\mathcal{S} \begin{bmatrix} u^+(\cdot, 0) \\ u^-(\cdot, L) \end{bmatrix} = \begin{bmatrix} \mathcal{S}_{11} & \mathcal{S}_{12} \\ \mathcal{S}_{21} & \mathcal{S}_{22} \end{bmatrix} \begin{bmatrix} u^+(\cdot, 0) \\ u^-(\cdot, L) \end{bmatrix} = \begin{bmatrix} u^-(\cdot, 0) \\ u^+(\cdot, L) \end{bmatrix}.$$

When the Helmholtz equation (1) is considered on domain Ω (i.e., one period of the waveguide), $u^+(x, 0)$ is the incident wave given in $z < 0$ and $u^-(x, L)$ is the incident wave given in $z > L$. If there is only an incident wave in $z < 0$, i.e., $u^-(x, L) = 0$, then the reflected wave is given by $u^-(x, 0) = \mathcal{S}_{11} u^+(x, 0)$ and the transmitted wave is given by $u^+(x, L) = \mathcal{S}_{21} u^+(x, 0)$. Therefore, $\mathcal{S}_{11}$ and $\mathcal{S}_{21}$ are the reflection and transmission operators for incident waves given in $z < 0$. Similarly, $\mathcal{S}_{22}$ and $\mathcal{S}_{12}$ are the reflection and transmission operators for incident waves given in $z > L$. Now if u is a Bloch mode given in (3), the quasi-periodic condition (5) implies that

$$u^+(x, L) = \rho\, u^+(x, 0), \quad u^-(x, L) = \rho\, u^-(x, 0).$$

This gives rise to the following eigenvalue problem:

$$\begin{bmatrix} \mathcal{S}_{11} & -I \\ \mathcal{S}_{21} & 0 \end{bmatrix} \begin{bmatrix} u^+(\cdot, 0) \\ u^-(\cdot, 0) \end{bmatrix} = \rho \begin{bmatrix} 0 & -\mathcal{S}_{12} \\ I & -\mathcal{S}_{22} \end{bmatrix} \begin{bmatrix} u^+(\cdot, 0) \\ u^-(\cdot, 0) \end{bmatrix}. \tag{11}$$

If the x variable is truncated and discretized by K points, the operators $\mathcal{S}_{jk}$, for $j, k = 1, 2$, can be approximated by $K \times K$ matrices, the eigenvalue problem (11) is then reduced to a generalized matrix eigenvalue problem involving $(2K) \times (2K)$ matrices. A matrix approximation to (11) can also be obtained if we expand the field in a truncated series. We can use expansions on the eigenmodes of the transverse operator $\partial_x^2 + k_0^2 n^2$ or simply a Fourier series. If K terms are retained for each field components, we also obtain an eigenvalue problem of $(2K) \times (2K)$ matrices.

In the transfer matrix reformulation based on forward and backward wave field components, we have a transfer matrix operator $\mathcal{T}$ satisfying

$$\mathcal{T} \begin{bmatrix} u^+(\cdot, 0) \\ u^-(\cdot, 0) \end{bmatrix} = \begin{bmatrix} u^+(\cdot, L) \\ u^-(\cdot, L) \end{bmatrix}.$$

Then the eigenvalue problem for a Bloch mode is simply

$$\mathcal{T} \begin{bmatrix} u^+(\cdot, 0) \\ u^-(\cdot, 0) \end{bmatrix} = \rho \begin{bmatrix} u^+(\cdot, 0) \\ u^-(\cdot, 0) \end{bmatrix}. \tag{12}$$

Clearly, $\mathcal{T}$ is related to $\mathcal{S}$ by

$$\mathcal{T} = \begin{bmatrix} 0 & -\mathcal{S}_{12} \\ I & -\mathcal{S}_{22} \end{bmatrix}^{-1} \begin{bmatrix} \mathcal{S}_{11} & -I \\ \mathcal{S}_{21} & 0 \end{bmatrix}.$$

However, it is numerical unstable to find the operator T directly.

For one period of the waveguide, i.e. Ω, the DtN map $\mathcal{M}$ is the a 2×2 matrix with operator entries satisfying

$$\mathcal{M}\begin{bmatrix} u(\cdot,0) \\ u(\cdot,L) \end{bmatrix} = \begin{bmatrix} \mathcal{M}_{11} & \mathcal{M}_{12} \\ \mathcal{M}_{21} & \mathcal{M}_{22} \end{bmatrix} \begin{bmatrix} u(\cdot,0) \\ u(\cdot,L) \end{bmatrix} = \begin{bmatrix} \partial_y u(\cdot,0) \\ \partial_y u(\cdot,L) \end{bmatrix}. \tag{13}$$

The DtN map $\mathcal{M}$ gives another reformulation of the eigenvalue problem of PCWs. For a Bloch mode, the quasi-periodic condition (6) immediately gives rise to

$$\begin{bmatrix} \mathcal{M}_{11} & -I \\ \mathcal{M}_{21} & 0 \end{bmatrix} \begin{bmatrix} u(\cdot,0) \\ \partial_y u(\cdot,0) \end{bmatrix} = \rho \begin{bmatrix} -\mathcal{M}_{12} & 0 \\ -\mathcal{M}_{22} & I \end{bmatrix} \begin{bmatrix} u(\cdot,0) \\ \partial_y u(\cdot,0) \end{bmatrix}, \tag{14}$$

where ρ is the eigenvalue. Similar to the scattering operator formalism, when K points are used to discretize x, we obtain a generalized matrix eigenvalue problem of $(2K)\times(2K)$ matrices.

A transfer matrix reformulation based on the total fields is also possible. Consider the 2×2 matrix operator $\mathcal{N}$ satisfying

$$\mathcal{N}\begin{bmatrix} u(\cdot,0) \\ \partial_y u(\cdot,0) \end{bmatrix} = \begin{bmatrix} u(\cdot,L) \\ \partial_y u(\cdot,L) \end{bmatrix},$$

we immediately have the following eigenvalue problem for Bloch modes

$$\mathcal{N}\begin{bmatrix} u(\cdot,0) \\ \partial_y u(\cdot,0) \end{bmatrix} = \rho \begin{bmatrix} u(\cdot,0) \\ \partial_y u(\cdot,0) \end{bmatrix}. \tag{15}$$

A simple relationship between $\mathcal{N}$ and $\mathcal{M}$ exists, but it is again numerically unstable to calculate $\mathcal{N}$.

Although the reformulations (11) and (14) give rise to linear eigenvalue value problems of smaller matrices, they are useful only if the scattering operator $\mathcal{S}$ or the DtN map $\mathcal{M}$ can be efficiently calculated. A number of different numerical methods have been developed to calculate $\mathcal{S}$ and $\mathcal{M}$. The finite element method has been used in [29] and [31], but it requires a discretization of Ω, same as the finite element method formulated on Ω directly. The Fourier modal method and a finite difference modal method have also been used to find $\mathcal{S}$ and $\mathcal{M}$ [30], respectively. These methods approximate Ω by many y-invariant segments and calculate local eigenmodes for each segment, but their accuracy is limited by the "staircase" approximation to dielectric interfaces. The scattering operator can also be calculated by the multipole method [26,27]. Since the transverse direction is assumed to be periodic on a larger scale in the "supercell" approach, the multipole method requires sophisticated lattice sums techniques. In the next section, we develop a simple and efficient method for calculating the DtN map $\mathcal{M}$. Together with the reformulation (14), we obtain an efficient method for analyzing PCWs.

3. Dirichlet-to-Neumann maps

The domain Ω given in (7) covers one period of the PCW along the waveguide axis and it is unbounded in the transverse direction. For practical numerical calculations, we have to truncate the transverse variable x to a finite interval, say $x_0 < x < x_J$. This gives rise to the rectangular domain

$$\hat{\Omega} = \{(x, y) \,|\, x_0 < x < x_J,\, 0 < y < L\}.$$

For a true propagating mode, the Bloch wavenumber β is real and the mode profile decays rapidly to zero as $x \to \pm\infty$. Therefore, accurate approximation to the propagating modes can be obtained if the truncated domain $\hat{\Omega}$ is moderately large in the x direction. In the standard "supercell" approach, due to the use of Fourier series in both x and y directions, the original PCW structure is replaced by a structure that duplicates $\hat{\Omega}$ periodically in the x direction. Standard techniques developed for calculating band structures of PhCs can thus be applied with $\hat{\Omega}$ as the unit cell. In the following, we use a simple zero boundary condition at x_0 and x_J. For convenience, we still call $\hat{\Omega}$ the supercell, although our treatment of the boundary condition is different. The effect of truncating the domain Ω with a zero boundary condition will be studied in numerical experiments.

For the supercell $\hat{\Omega}$, the DtN map $\mathcal{M}$ is the operator satisfying (13) for all solutions of the Helmholtz equation (1) subject to the additional zero boundary condition:

$$u(x, y) = 0, \quad x = x_0 \;\text{ and }\; x = x_J.$$

We assume that $\hat{\Omega}$ consists of J square or rectangular elementary cells each containing at most one cylinder. More precisely, we have $x_0 < x_1 < x_2 < ... < x_J$, so that $\hat{\Omega}$ is the union of Ω_1, Ω_2, ..., Ω_J, where Ω_j is given by $x_{j-1} < x < x_j$ and $0 < y < L$. To calculate $\mathcal{M}$, we first have to find the DtN maps of the elementary cells. For Ω_j, the DtN map $\Lambda^{(j)}$ satisfies:

$$\Lambda^{(j)} \begin{bmatrix} u_{0j} \\ v_{j-1} \\ v_j \\ u_{1j} \end{bmatrix} = \begin{bmatrix} \Lambda^{(j)}_{11} & \Lambda^{(j)}_{12} & \Lambda^{(j)}_{13} & \Lambda^{(j)}_{14} \\ \Lambda^{(j)}_{21} & \Lambda^{(j)}_{22} & \Lambda^{(j)}_{23} & \Lambda^{(j)}_{24} \\ \Lambda^{(j)}_{31} & \Lambda^{(j)}_{32} & \Lambda^{(j)}_{33} & \Lambda^{(j)}_{34} \\ \Lambda^{(j)}_{41} & \Lambda^{(j)}_{42} & \Lambda^{(j)}_{43} & \Lambda^{(j)}_{44} \end{bmatrix} \begin{bmatrix} u_{0j} \\ v_{j-1} \\ v_j \\ u_{1j} \end{bmatrix} = \begin{bmatrix} \partial_y u_{0j} \\ \partial_x v_{j-1} \\ \partial_x v_j \\ \partial_y u_{1j} \end{bmatrix}, \tag{16}$$

where $u_{0j} = u(x, 0)$ and $u_{1j} = u(x, L)$ for $x_{j-1} < x < x_j$, $v_{j-1} = u(x_{j-1}, y)$ and $v_j = u(x_j, y)$ for $0 < y < L$, $\partial_y u_{0j} = \partial_y u(x, 0)$, $\partial_x v_j = \partial_x u(x_j, y)$, etc. We have written $\Lambda^{(j)}$ in a 4×4 block form in accordance with the four edges of Ω_j. The operator $\Lambda^{(j)}$ can be approximated by a matrix. If we choose N_x points for each horizontal edge (i.e. for $x_{j-1} < x < x_j$ at $y = 0$ or $y = L$) and N_y points for each vertical edge (i.e. for $0 < y < L$ at $x = x_{j-1}$ or $x = x_j$), then $\Lambda^{(j)}$ can be approximated by a $N_t \times N_t$ matrix, where $N_t = 2(N_x + N_y)$. As described in [35, 38], we start with assuming that the general solution of the Helmholtz equation in Ω_j

can be approximated by a linear combination of N_t special solutions:

$$u(x,y) = \sum_{k=1}^{N_t} c_k \phi_k(x,y), \tag{17}$$

where ϕ_k is a cylindrical wave given analytically if Ω_j contains a circular cylinder at the center. If Ω_j is homogeneous, ϕ_k can be either a plane wave or a cylindrical wave. If we evaluate (17) at the N_t sampling points on the edges of Ω_j, we have a matrix $\mathcal{A}$ that maps the coefficients $\{c_k\}$ to the values of u at these N_t points. We can also evaluate the normal derivative of u at the N_t sampling points on the boundary of Ω_j. This gives rise to another matrix $\mathcal{B}$ that maps $\{c_k\}$ to the normal derivatives of u at the N_t points. Finally, the DtN map is approximated by

$$\Lambda^{(j)} = \mathcal{B}\mathcal{A}^{-1}.$$

Typically, we choose N_x and N_y such that x and y are sampled at $\{\xi_k\}$ and $\{\eta_l\}$, respectively, where

$$\begin{aligned} \xi_k &= x_{j-1} + (k-0.5)\frac{x_j - x_{j-1}}{N_x}, \quad k = 1, 2, ..., N_x, \\ \eta_l &= (l-0.5)\frac{L}{N_y}, \quad l = 1, 2, ..., N_y. \end{aligned}$$

In that case, u_{0j} and u_{1j} are column vectors of length N_x, v_{j-1} and v_j are column vectors of length N_y, $\Lambda_{11}^{(j)}$ is a $N_x \times N_x$ matrix, $\Lambda_{12}^{(j)}$ is a $N_x \times N_y$ matrix, etc. Since the size of the elementary cells is typically smaller than the free space wavelength, it is usually sufficient to choose N_x and N_y to be less than 10. Finally, we notice that the DtN maps of elementary cells with the same refractive index profile are identical. Therefore, we only have to calculate the DtN maps for cells with distinct profiles. For PCWs constructed from removing one or more rows of cylinders in an otherwise perfectly periodic PhC, we only have two different types of elementary cells: the ordinary cell with one cylinder inside and the defect cell of a homogeneous medium.

The DtN map $\mathcal{M}$ of the supercell $\hat{\Omega}$ can be obtained from merging the DtN maps of the elementary cells. This is essentially a process of elimination where the vertical edges (for v_1, v_2, ..., v_{J-1}) are eliminated using the DtN maps $\Lambda^{(j)}$ and the continuity of $\partial_x u$. Since a zero boundary condition is assumed at x_0 and x_J, we have $v_0 = v_J = 0$. Let us introduce the column vectors u_0, u_1 and v as follows:

$$u_0 = \begin{bmatrix} u_{01} \\ u_{02} \\ \vdots \\ u_{0J} \end{bmatrix}, \quad u_1 = \begin{bmatrix} u_{11} \\ u_{12} \\ \vdots \\ u_{1J} \end{bmatrix}, \quad v = \begin{bmatrix} v_1 \\ v_2 \\ \vdots \\ v_{J-1} \end{bmatrix}.$$

Here, v is a vector of length $(J-1)N_y$ representing the field u at the sampling points on the vertical edges at x_1, x_2, ..., x_{J-1}. The vectors u_0 and u_1 represent u at the sampling points on the horizontal edges of $\hat{\Omega}$ at $y = 0$ and $y = L$, respectively. Let K be the total number of sampling points on each horizontal edge of $\hat{\Omega}$, then u_0 and u_1 are vectors of length K. If N_x is a constant for all elementary cells, then $K = JN_x$. For the vertical edge at x_j, we can use the DtN maps of Ω_j and Ω_{j+1} to evaluate $\partial_x v_j = \partial_x u(x_j, y)$. That is

$$\begin{aligned}\partial_x v_j &= \Lambda_{31}^{(j)} u_{0j} + \Lambda_{32}^{(j)} v_{j-1} + \Lambda_{33}^{(j)} v_j + \Lambda_{34}^{(j)} u_{1j} \\ &= \Lambda_{21}^{(j+1)} u_{0,j+1} + \Lambda_{22}^{(j+1)} v_j + \Lambda_{23}^{(j+1)} v_{j+1} + \Lambda_{24}^{(j+1)} u_{1,j+1}.\end{aligned}$$

Therefore,

$$\begin{aligned}&\Lambda_{32}^{(j)} v_{j-1} + (\Lambda_{33}^{(j)} - \Lambda_{22}^{(j+1)}) v_j - \Lambda_{23}^{(j+1)} v_{j+1} \\ &= -\Lambda_{31}^{(j)} u_{0j} + \Lambda_{21}^{(j+1)} u_{0,j+1} - \Lambda_{34}^{(j)} u_{1j} + \Lambda_{24}^{(j+1)} u_{1,j+1}.\end{aligned}$$

The above is a relationship between the wave fields on the seven edges of two neighboring elementary cells Ω_j and Ω_{j+1}. We can put such relationships for all j $(1 \le j < J)$ in the following equation:

$$\mathcal{C}_0 v = \mathcal{C}_1 \begin{bmatrix} u_0 \\ u_1 \end{bmatrix}, \tag{18}$$

where $\mathcal{C}_0$ is a square block tridiagonal matrix, and solve for v:

$$v = \mathcal{C}_0^{-1} \mathcal{C}_1 \begin{bmatrix} u_0 \\ u_1 \end{bmatrix}.$$

On the other hand, we can evaluate the y derivative of u_{0j} and u_{1j} by the DtN map $\Lambda^{(j)}$. From the first and last rows of (16), we have

$$\frac{\partial}{\partial y} \begin{bmatrix} u_{0j} \\ u_{1j} \end{bmatrix} = \begin{bmatrix} \Lambda_{11}^{(j)} & \Lambda_{14}^{(j)} \\ \Lambda_{41}^{(j)} & \Lambda_{44}^{(j)} \end{bmatrix} \begin{bmatrix} u_{0j} \\ u_{1j} \end{bmatrix} + \begin{bmatrix} \Lambda_{12}^{(j)} & \Lambda_{13}^{(j)} \\ \Lambda_{42}^{(j)} & \Lambda_{43}^{(j)} \end{bmatrix} \begin{bmatrix} v_{j-1} \\ v_j \end{bmatrix}.$$

This gives rise to matrices $\mathcal{D}_0$ and $\mathcal{D}_1$, such that

$$\frac{\partial}{\partial y} \begin{bmatrix} u_0 \\ u_1 \end{bmatrix} = \mathcal{D}_0 \begin{bmatrix} u_0 \\ u_1 \end{bmatrix} + \mathcal{D}_1 v. \tag{19}$$

Thus

$$\frac{\partial}{\partial y} \begin{bmatrix} u_0 \\ u_1 \end{bmatrix} = \left(\mathcal{D}_0 + \mathcal{D}_1 \mathcal{C}_0^{-1} \mathcal{C}_1 \right) \begin{bmatrix} u_0 \\ u_1 \end{bmatrix}.$$

Therefore, the DtN map of $\hat{\Omega}$ is approximated by the matrix

$$\mathcal{M} = \mathcal{D}_0 + \mathcal{D}_1 \mathcal{C}_0^{-1} \mathcal{C}_1. \tag{20}$$

The size of the matrix $\mathcal{M}$ is $(2K) \times (2K)$. If we partition $\mathcal{M}$ in 2×2 blocks, we can then find the Bloch modes of the PCW by solving the generalized eigenvalue problem (14) using standard linear algebra programs.

4. Numerical examples

To illustrate our DtN mode solver, we consider two examples. The first example has been previously analyzed by Yu and Chang [11] using a frequency domain finite difference method. The PhC is a square lattice of dielectric cylinders with dielectric constant $\epsilon_1 = n_1^2 = 10$ and radius $r = 0.375L$, where L is the lattice constant. The background medium is air. The PCW is formed by removing one row of cylinders as in Fig. 1. The supercell $\hat{\Omega}$ is composed of one defect cell and $2m$ regular elementary cells (with m cells at each side of the line defect), so that $J = 2m + 1$, $x_J = -x_0 = (m + 0.5)L$ and $x_j - x_{j-1} = L$. For each elementary cell, the DtN map $\Lambda^{(j)}$ is obtained with $N = N_x = N_y$ sampling points on each edge, so that the total number of sampling points on a horizontal edge of $\hat{\Omega}$ is $K = JN = (2m + 1)N$. In Fig. 2 we

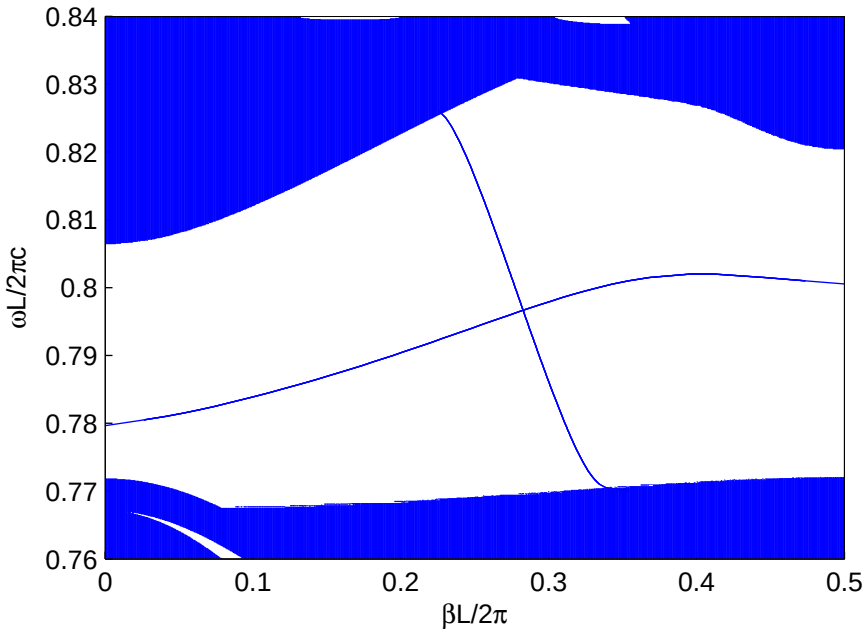

Fig. 2. Dispersion curves (for the E polarization) of a photonic crystal waveguide composed of one missing row in a square lattice of dielectric rods.

show the dispersion curves of the propagating modes for both polarizations obtained with $N = 7$ and $m = 10$. The shadowed region indicates those β and ω, such that the photonic crystal without the line defect has a Bloch wave solution

$$u(x, y) = e^{i(\alpha x + \beta y)} \Phi(x, y)$$

for a real α and a function Φ which is periodic in both x and y with period L. The waveguide modes can be classified as odd and even based on their symmetry. Our results are in good

agreement with those of Yu and Chang [11]. We have also repeated the calculations with $m = 16$ and obtained nearly identical results. For the E polarization and the normalized frequency $\omega L/(2\pi c) = 0.8$, we plot the electric field patterns of the propagating modes in Fig. 3. It is clear that modes are well confined around the defect cell at the center. We also

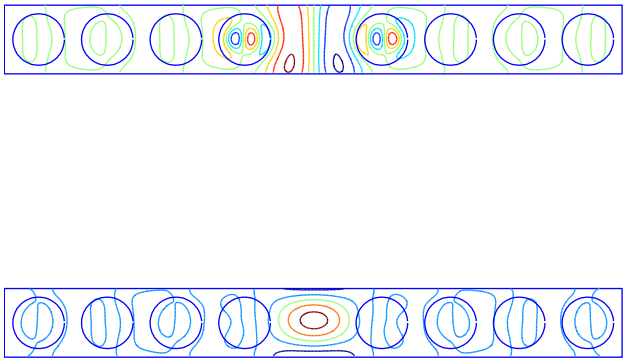

Fig. 3. Electric field patterns of the propagating modes (E polarization) of a photonic crystal waveguide at $\omega L/(2\pi c) = 0.8$. The top and the bottom figures are the odd and even modes, respectively, and their Bloch wavenumbers are $\beta L/(2\pi) = 0.3346$ and 0.2773.

check the convergence of our method with respect to N. For $m = 10$, $\omega L/(2\pi c) = 0.8$ and the even mode, we calculate the propagation constant β for $4 \le N \le 19$, and use the result obtained with $N = 19$ as a reference solution to calculate the following approximate relative error:

$$E_N = |\beta^{(N)} - \beta^{(19)}|/|\beta^{(19)}|,$$

where $\beta^{(N)}$ denotes β obtained with N sampling points on each edge of the elementary cells. As shown in Fig. 4, the relative errors appear to decrease exponentially. Apparently, the results are more accurate when N is an odd integer. In that case, the center of each edge is one of the sampling points where the normal derivative of the field is matched and this may have led to the higher accuracy.

For the case of $N = 7$ and $m = 10$, we have $J = 147$ and the eigenvalue problem (14) involves 294×294 matrics. We have implemented our method in MATLAB. On a PC with a 3.4GHz Pentium 4 CPU and 2GB of RAM running the Linux operating system, the required time to compute the Bloch wavenumber β at a given frequency is about 2 seconds. This

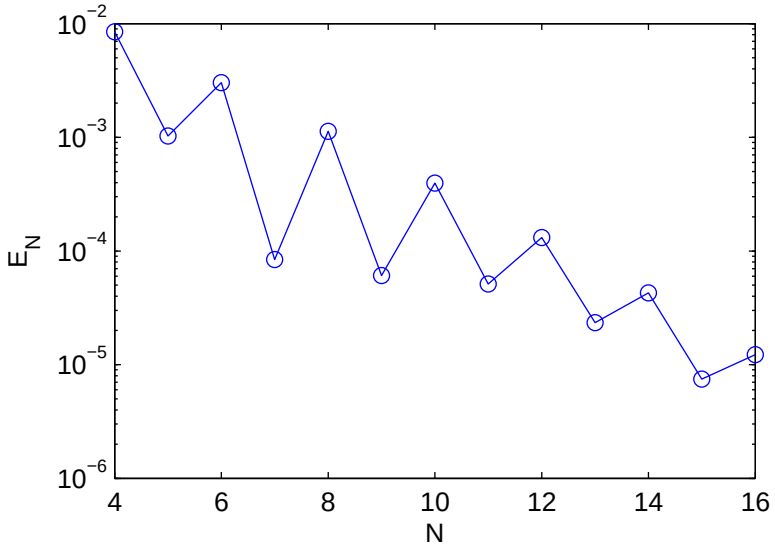

Fig. 4. Relative error E_N of the propagation constant β of a photonic crystal waveguide obtained with a reference solution at $N = 19$.

includes 0.1 seconds to setup the matrix $\mathcal{M}$ and 1.85 seconds to find all eigenvalues of (14) to full precision. If there is a good initial guess for the Bloch wavenumber β, which is the case when we have already solved the problem for a nearby frequency, we can calculate only the desired eigenvalue of (14) by the inverse iteration method using less than 1 second. For comparison, we use the plane wave expansion (PWE) method as implemented in the MIT Photonic-Bands package [16]. Corresponding to $m = 10$, the supercell contains 21 elementary unit cells. With 16 plane waves for each lattice constant, the PWE method gives rise to a 5376×5376 matrix. Using the targeted-frequency feature of the MIT Photonic-Bands package and a reduced error tolerance of 10^{-5}, we can calculate the defect mode frequency for a given Bloch wavenumber in 2 to 3 minutes on the same computer. However, the accuracy is limited. As an example, we consider the solution at $\omega L/(2\pi c) = 0.8$ and $\beta L/(2\pi) = 0.2773$. If we specify $\beta L/(2\pi) = 0.2773$ as an input and $\omega L/(2\pi c) = 0.8$ as the target frequency, the PWE method gives the defect mode frequency at $\omega L/(2\pi c) = 0.803$. When the number of plane waves for each lattice constant is increased to 32, the PWE method gives the correct defect mode frequency to three significant digits, i.e. $\omega L/(2\pi c) = 0.800$. In that case, the method produces a 21504×21504 matrix and requires 8 to 12 minutes to find the defect mode frequency for a given Bloch wavenumber and a target frequency.

The second example, as depicted in Fig. 5, has been previously studied by Adibi *et al.* [7] and Yu and Chang [11] using finite difference methods in time and frequency domains, respectively. The waveguide is formed by six arrays of circular air holes in a dielectric slab

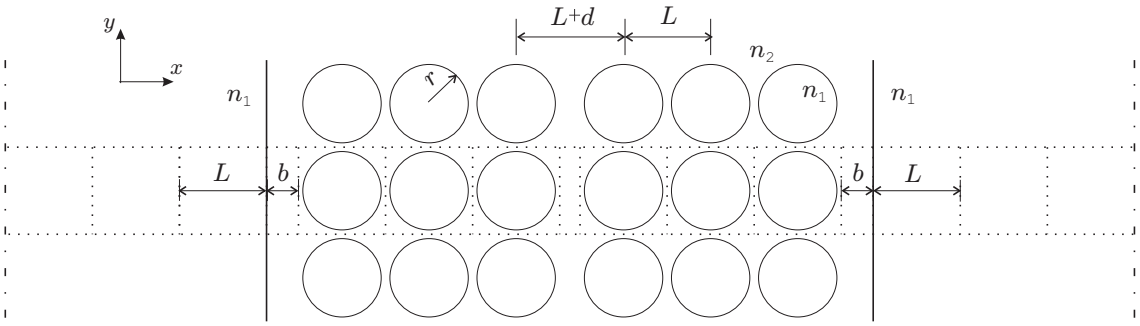

Fig. 5. A photonic crystal waveguide composed of air holes in a finite dielectric slab.

with refractive index $n_2 = 3.6$. The air holes form a square lattice with a lattice constant L, except that the distance between the third and fourth arrays is increased by $d = 0.375L$. The radius of the air holes is $r = 0.45L$. The background dielectric slab is finite in the x direction with a total thickness of $6L + d + 2b$, where $b = (5/12)L$ is the thickness of extra dielectric medium outside the first and sixth arrays. The dielectric slab is surrounded by air. We consider the propagating modes of this waveguide in the E polarization. As given in [7], a bandgap for such a infinite square lattice of air holes in the dielectric medium is $0.216 < \omega L/(2\pi c) < 0.248$.

In our calculations, we truncate the x variable at a distance of mL away from the edges of the slab, where m is a positive integer. The supercell $\hat{\Omega}$ consists of $J = 2m + 9$ elementary cells. Outside the slab, we have m square air cells of size $L \times L$ for both positive and negative directions of x. Inside the slab, we have 6 square cells each containing one air hole, one rectangular cell of size $d \times L$ at the center of the structure and two rectangular cells of size $b \times L$ at the edges of the slab. This gives rise to $x_0 < x_1 < ... < x_J$ satisfying

$$x_J = -x_0 = (m+3)L + \frac{d}{2} + b,$$
$$x_{j+1} - x_j = \begin{cases} b & \text{if } j = m \text{ and } j = m+8, \\ d & \text{if } j = m+4, \\ L & \text{otherwise.} \end{cases}$$

Four different types of elementary cells are involved in the supercell. Fig. 6 gives the dispersion curves calculated using our DtN mode solver with $N = 8$ and $m = 4$. We have repeated the calculations with $m = 12$ and obtained nearly identical results. To the left of the light line, we have a region for the continuous spectrum. Since the average refractive index of the bulk crystal is less than that of the guiding slab, but still larger than that of the cladding air, both bandgap and index confinement effects contribute to the guiding mechanism. In Fig. 7, we show the mode profiles at the normalized frequency $\omega L/(2\pi c) = 0.23$. Ordered

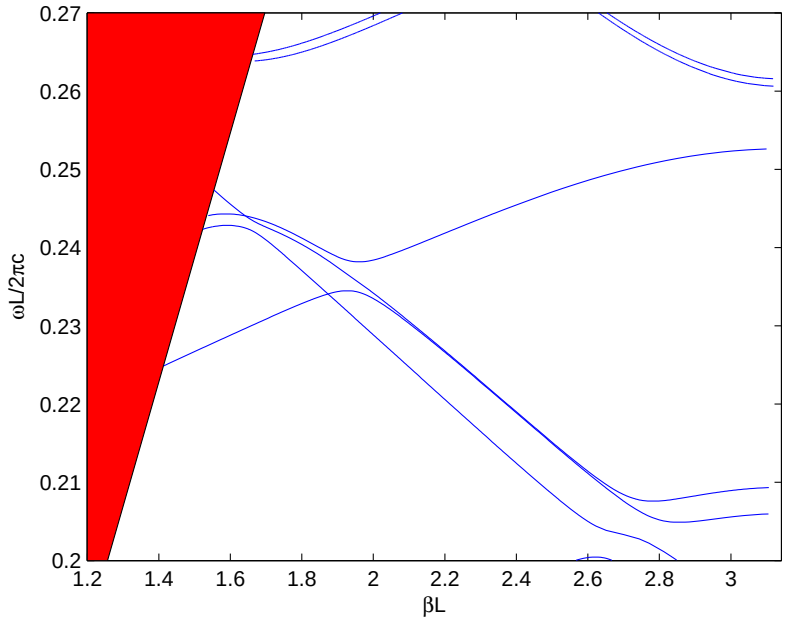

Fig. 6. Dispersion curves of the photonic crystal waveguide depicted in Fig. 5.

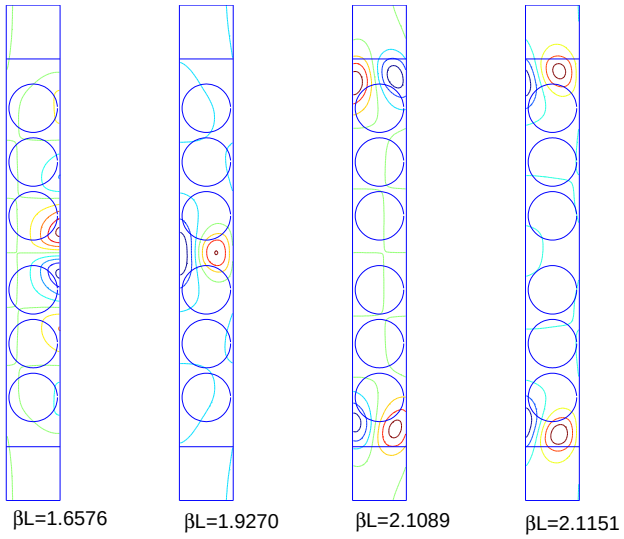

Fig. 7. Electric field patterns of the propagating modes (E polarization) for the photonic crystal waveguide depicted in Fig. 5 and $\omega L/(2\pi c) = 0.23$.

by their values of β, the first and second modes are well confined at the central dielectric region and they are odd and even with respect to the waveguide axis $y = 0$, respectively, The other two modes concentrate on the edges of the dielectric slab. In earlier studies [7,11], only the second mode is obtained, probably due to the use of a perfectly matched layer (PML) immediately next to the dielectric slab. The third and fourth modes have large field intensities near the edges of the slab, and they will be significantly distorted by the PMLs. Although the modes confined near the waveguide core are more important, it is necessary to realize the multi-mode nature of this waveguide.

5. Conclusion

In this paper, we developed an efficient numerical method for analyzing photonic crystal waveguides based on the Dirichlet-to-Neumann (DtN) map of the supercell. Our method is suitable for two-dimensional photonic crystals composed of circular cylinders. The starting point is the construction of DtN maps of the elementary unit cells by cylindrical wave expansions. These DtN maps of the elementary cells are used to build the DtN map of the supercell of the waveguide. The waveguide modes are then solved from a linear eigenvalue problem formulated on the boundaries of the supercell using the DtN map. Compared with other methods, our method gives rise to matrices of smaller size. Numerical examples indicate a fast convergence with respect to the number of sampling points on each edge of the elementary cells. Since the sizes of the elementary unit cells are typically smaller than the wavelength, to obtain three or four significant digits in the solution, only a small number of sampling points, such as 7 or 9, are needed on each edge of the unit cells. Furthermore, it appears that an odd number of points on each edge gives more accurate results.

Acknowledgments

This research was partially supported by a City University of Hong Kong research grant (Project No. 7002131).

Ya Yan Lu's e-mail address is mayylu@cityu.edu.hk.

References

1. E. Yablonovitch, "Inhibited spontaneous emission in solid-state physics and electronics", Phys. Rev. Lett. **58**, 2059-2062 (1987).
2. S. John, "Strong localization of photons in certain disordered dielectric superlattices", Phys. Rev. Lett. **58**, 2486-2489 (1987).
3. J. D. Joannopoulos, R. D. Meade and J. N. Winn, *Photonic Crystals: Molding the Flow of Light*, (Princeton University Press, Princeton, NJ. 1995).

4. A. Mekis, J. C. Chen, I. Kurland, S. H. Fan, P. R. Villeneuve and J. D. Joannopoulos, "High transmission through sharp bends in photonic crystal waveguides", Phys. Rev. Lett. **77**, 3787-3790 (1996).
5. K. Sakoda, T. Ueta and K. Ohtaka, "Numerical analysis of eigenmodes localized at line defects in photonic lattices", Phys. Rev. B **56**, 14905-14908 (1997).
6. M. Qiu and S. L. He, "Guided modes in a two-dimensional metallic photonic crystal waveguide", Physics Letters A **266**, 425-429 (2000).
7. A. Adibi, Y. Xu, R. K. Lee, A. Yariv and A. Scherer, "Properties of the slab modes in photonic crystal optical waveguides", J. Lightw. Technol. **18**, 1554-1564 (2000).
8. H. Benisty, "Modal analysis of optical guides with two-dimensional photonic band-gap boundaries", Journal of Applied Physics **79**, 7483-7492 (1996).
9. R. Zoli, M. Gnan, D. Castaldini, G. Bellanca and P. Bassi, "Reformulation of the plane wave method to model photonic crystals", Opt. Express **11**, 2905-2910 (2003).
10. A. David, H. Benisty and C. Weisbuch, "Fast factorization rule and plane-wave expansion method for two-dimensional photonic crystals with arbitrary hole-shape", Phys. Rev. B **73**, 075107 (2006).
11. C. P. Yu and H. C. Chang, "Applications of the finite difference mode solution method to photonic crystal structures", Opt. Quant. Electron. **36**, 145-163 (2004).
12. R. D. Meade, A. M. Rappe, K. D. Brommer, J. D. Joannopoulos and O. L. Alerhand, "Accurate theoretical analysis of photonic band-gap materials", Phys. Rev. B **48,** 8434-8437 (1993).
13. H. Y. D. Yang, "Finite difference analysis of 2-D photonic crystals", IEEE Trans. Microwave Theory Tech. **44,** 2688-2695 (1996).
14. D. C. Dobson, "An efficient method for band structure calculations in 2D photonis crystals", J. Comput. Phys. **149**, 363-379 (1999).
15. W. Axmann and P. Kuchment, "An efficient finite element method for computing spectra of photonic and acoustic band-gap materials: I. Scalar case", J. Comput. Phys. **150**, 468-481 (1999).
16. S. G. Johnson and J. D. Joannopoulos, "Block-iterative frequency-domain methods for Maxwell's equations in a planewave basis", Opt. Express **8**, 173-190 (2001).
17. E. Moreno, D. Erni and C. Hafner, "Band structure computations of metallic photonic crystals with the multiple multipole method", Phys. Rev. B **65**, 155120 (2002).
18. M. Marrone, V. F. Rodriguez-Esquerre and H. E. Hernández-Figueroa, "Novel numerical method for the analysis of 2D photonic crystals: the cell method", Opt. Express **10**, 1299-1304 (2002).
19. S. Jun, Y. S. Cho and S. Im, "Moving least-square method for the band-structure calculation of 2D photonic crystals", Opt. Express **11**, 541-551 (2003).

20. C. P. Yu and H. C. Chang, "Compact finite-difference frequency-domain method for the analysis of two-dimensional photonic crystals", Opt. Express **12**, 1397-1408 (2004).
21. S. Guo, F. Wu, S. Albin and R. S. Rogowski, "Photonic band gap analysis using finite-difference frequency-domain method", Opt. Express **12**, 1741-1746 (2004).
22. X. Checoury and J. M. Lourtioz, "Wavelet method for computing band diagrams of 2D photonic crystals", Opt. Commun. **259**, 360-365 (2006).
23. P. J. Chiang, C. P. Yu and H. C. Chang, "Analysis of two-dimensional photonic crystals using a multidomain pseudospectral method", Phys. Rev. E **75**, 026703 (2007).
24. S. Y. Shi, C. H. Chen and D. W. Prather, "Revised plane wave method for dispersive material and its application to band structure calculations of photonic crystal slabs", Appl. Phys. Lett. **86**, 43104 (2005).
25. J. B. Pendry, "Calculating photonic band structure", *Journal of Physics: Condensed Matter* **8,** 1085-1108 (1996).
26. L. C. Botten, N. A. Nicorovici, R. C. McPhedran, C. M. de Sterke and A. A. Asatryan, "Photonic band structure calculations using scattering matrices", Phys. Rev. E **64,** 046603 (2001).
27. K. Yasumoto, H. Jia and K. Sun, "Rigorous modal analysis of two-dimensional photonic crystal waveguides", Radio Science **40**, RS6S02 (2005).
28. H. Jia and K. Yasumoto, "Rigorous analysis of guided modes of two-dimensional metallic electromagnetic crystal waveguides", Journal of Electromagnetic Waves and Applications **19**, 1919-1933 (2005).
29. K. Dossou, M. A. Byrne and L. C. Botten, "Finite element computation of grating scattering matrices and application to photonic crystal band calculations", J. Comput. Phys. **219**, 120-143 (2006).
30. S. F. Helfert, "Numerical stable determination of Floquet-modes and the application to the computation of band structures", Opt. Quant. Electron. **36**, 87-107 (2004).
31. P. Joly, J.-R. Li and S. Fliss, "Exact boundary conditions for periodic waveguides containing a local perturbation", Commun. Comput. Phys. **1**, 945-973 (2006).
32. M. J. Grote and J. B. Keller, "On nonreflecting boundary conditions", J. Comput. Phys. **122**, 231-243 (1995).
33. J. Tausch and J. Butler, "Floquet multipliers of periodic waveguides via Dirichlet-to-Neumann maps", J. Comput. Phys. **159**, 90-102 (2000).
34. J. Tausch and J. Butler, "Efficient analysis of periodic dielectric waveguides using Dirichlet-to-Neumann maps", J. Opt. Soc. Am. A **19**, 1120-1128 (2002).
35. Y. X. Huang and Y. Y. Lu, "Scattering from periodic arrays of cylinders by Dirichlet-to-Neumann maps,", J. Lightw. Technol. **24**, 3448-3453 (2006).
36. Y. X. Huang and Y. Y. Lu, "Modeling photonic crystals with complex unit cells

by Dirichlet-to-Neumann maps," Journal of Computational Mathematics **25**, 337-349 (2007).

37. S. J. Li and Y. Y. Lu, "Multipole Dirichlet-to-Neumann map method for photonic crystals with complex unit cells," J. Opt. Soc. Am. A **24**, 2438-2442 (2007).
38. J. H. Yuan and Y. Y. Lu, "Photonic bandgap calculations using Dirichlet-to-Neumann maps," J. Opt. Soc. Am. A **23**, 3217-3222 (2006).
39. J. H. Yuan and Y. Y. Lu, "Computing photonic band structures by Dirichlet-to-Neumann maps: The triangular lattice," Opt. Commun. **273**, 114-120 (2007).